Ultrasonic investigation of fluorite-type BaF_2:Cu and BaF_2:Ni crystals

N. Yu. Ofitserova[1], M. N. Sarychev[1], I. V. Zhevstovskikh[1,2], V. A. Ulanov[3], V. T. Surikov[4], N. S. Averkiev[5], V. V. Gudkov[1]

[1]*Ural Federal University, Ekaterinburg, Russia*

[2]*M. N. Mikheev Institute of Metal Physics, Ural Branch of Russian Academy of Sciences, Ekaterinburg, Russia*

[3] *E. K. Zavoisky Physical Technical Institute, FRC Kazan Scientific Centre of Russian Academy of Sciences, Kazan, Russia*

[4]*Institute of Solid State Chemistry, Ural Branch of Russian Academy of Sciences, Ekaterinburg, Russia*

[5]*A. F. Ioffe Physical Technical Institute of Russian Academy of Sciences, St. Petersburg, Russia*

n.ofitserova@mail.ru

Introduction

Transition metal ions with orbital degeneracy lead to the Jahn-Teller (JT) effect manifestation in crystals. The research relevance is determined by the possibilities of practical application of transition metal ions in quantum optics, spintronics, computer technology, solar cells and LEDs. If the ion is a Jahn –Teller center, the study of the ground state of JT-complexes will open an additional possibility to control the device in which these complexes are possible to use.

The present research is aimed at construction of the temperature dependence of relaxation time in fluorite crystals which provides the information about the parameters of relaxation mechanisms.

Crystal structure and local distortions

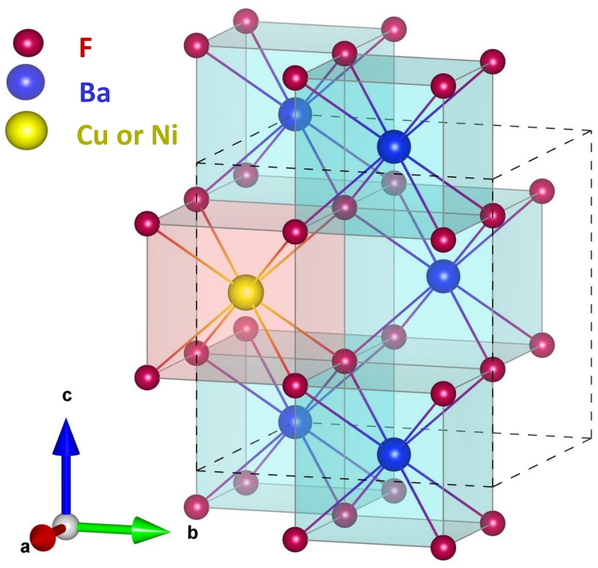

Fig.1 - Fluorite structure of the cubic BaF_2 crystal doped with Cu or Ni ions. The Cu (Ni) ions replaces Ba ion in the lattice site. It is surrounded by eight fluorine ions in the corners of the cube.

Cubic $Cu^{2+}F_8^-$ Jahn-Teller complex is determined by $T\otimes(e+t_2)$ problem with 6 orthorhombic global minima of the adiabatic potential energy surface [1].

Cu^{2+} ions in cubic environment are characterized by triple orbital degeneracy. Adiabatic potential energy surface is defined by 5 symmetric coordinates:

- tetragonal: $Q_\vartheta, Q_\varepsilon$,
- trigonal: Q_ξ, Q_η, Q_ζ [2].

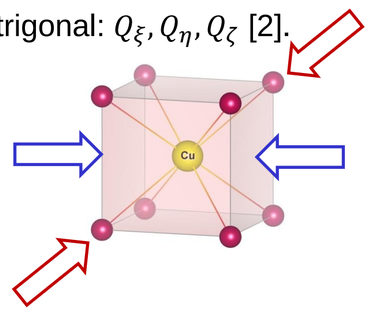

Fig.2 – Tetragonal e (blue) and trigonal t_2 (red) distortions. There is simultaneous interaction with both tetragonal and trigonal displacements in case of the $T\otimes(e+t_2)$ problem.

Acoustic experiment methodology

The ultrasonic waves with specific polarization propagated along the specific crystallographic axis fully characterize the elastic moduli of the crystal (Table 1).

In an ultrasonic experiment, temperature dependences of the ultrasound velocity v and attenuation α (Real and Imaginary components of complex elastic modulus, respectively) are registered.

$$\frac{\Delta c}{c_0} = 2\cdot\left(\frac{\Delta v}{v_0} + i\frac{\Delta\alpha}{k_0}\right) \qquad (1)$$

JT-subsystem contribution to elastic moduli is determined as peak in the Imaginary part and minimum in the Real part at $T\approx T_1$.

$$\frac{c^{JT}}{c_0} = 2\frac{\mathrm{Re}[c^{JT}(T_1)]}{c_0}\frac{T_1}{T}\frac{1}{1+(\omega\tau)^2} + 2i\frac{\mathrm{Im}[c^{JT}(T_1)]}{c_0}\frac{T_1}{T}\frac{\omega\tau}{1+(\omega\tau)^2} \qquad (2)$$

$$\mathrm{Re}[c^{JT}(T_1)] = -\mathrm{Im}[c^{JT}(T_1)] \qquad (3)$$

Experimental determination of the distortions and symmetric properties of global minima and saddle points (which are potential energy barriers tunneling passes through) is based on relaxation anomalies appearance in specific elastic moduli (Table 1).

Operation of experimental setup is based on the frequency-variable high-frequency bridge. Ultrasound waves are generated and registered using piezoelectric transducers made of $LiNbO_3$.

Table 1. – Relation between ultrasonic wave propagation, cubic crystal elastic moduli and JT-complex distortions

Ultrasonic wave propagation	Shear: *k* || [110] polarization || [001]	Longitudal: *k* || [110]	Shear: *k* || [110] polarization || $[1\bar{1}0]$
Elastic modulus	c_{44}	$\frac{c_{11}+c_{12}+2c_{44}}{2}$	$\frac{c_{11}-c_{12}}{2}$
Distortions	Trigonal t_2 (4 global minima)		Tetragonal e (3 global minima)
	Orthorhombic (6 global minima)		

Experimental data

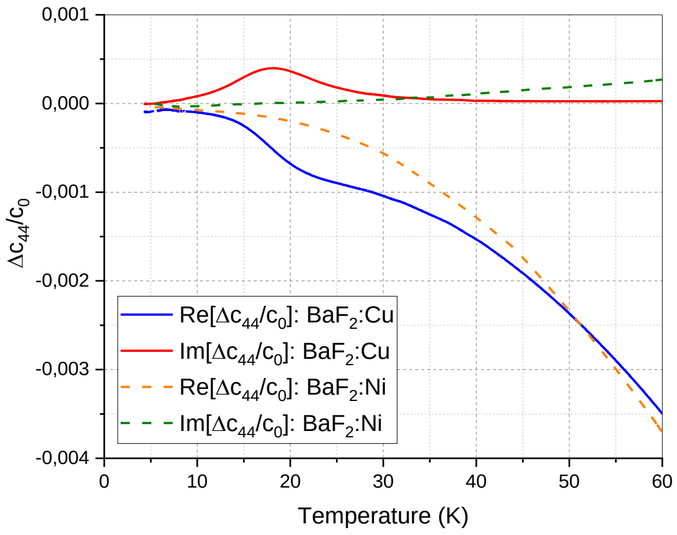

Results:

1. In BaF_2:Ni, there are no anomalies (visible signs of the Jahn-Teller effect).

2. In BaF_2:Cu, the peak in $\mathrm{Im}[\Delta c_{44}/c_0]$ and anomalies in $\mathrm{Re}[\Delta c_{44}/c_0]$ are much less than in $CaF_2:Cu^{2+}$ [1]. Therefore, only a small amount of the dopants does substitute metal in cation positions in BaF_2:Cu, others have off-centre positions which do not have the JT origin [3].

Fig.3 – Temperature dependences of Real and Imaginary parts of the c_{44} elastic modulus (share wave propagating along [110] axis polarized along [001] axis) in the BaF_2:Cu and BaF_2:Ni crystals at $\omega/2\pi$=53 MHz. $\Delta c_{44} = c_{44}(T) - c_0$, $c_0 = c_{44}(T_0)$; $T_0 = 4.8\ K$

Temperature dependence of relaxation time

Evaluation of relaxation time doesn't require concentration of the JT complexes and is based on the modeling the JT- contribution in Imaginary part of elastic modulus using fitting parameters and formula (2). Fitting parameters define three relaxation mechanisms:

activation: $\tau_a = \tau_0 exp(\frac{V_0}{T})$, tunneling: $\tau_t = \frac{1}{BT}$, two-phonon: $\tau_R = \frac{\Theta^2}{BT^3}$, $\frac{1}{\tau} = \frac{1}{\tau_a} + \frac{1}{\tau_t} + \frac{1}{\tau_R}$ (4)

Temperature dependence of relaxation time can be also determined using experimental data on the Imaginary part of elastic modulus using formula (5):

$$\tau = \frac{1}{\omega}\frac{\mathrm{Im}[c^{JT}(T_1)]T_1}{\mathrm{Im}[c^{JT}(T)]T} \pm \frac{1}{\omega}\sqrt{\left[\frac{\mathrm{Im}[c^{JT}(T_1)]T_1}{\mathrm{Im}[c^{JT}(T)]T}\right]^2 - 1} \qquad (5)$$

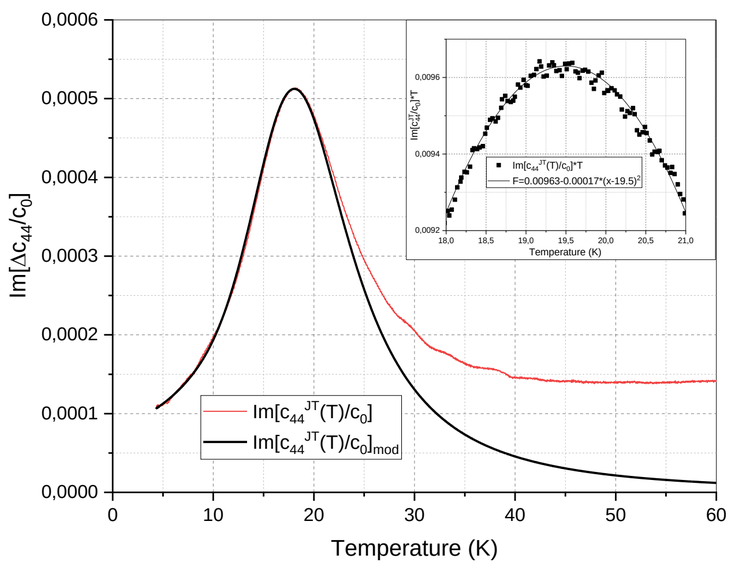

Fig.4 – Temperature dependences of the JT-contribution in the Imaginary part of the c_{44} elastic modulus in the BaF_2:Cu crystal: red curve is experimental curve $\mathrm{Im}[\Delta c_{44}(T)/c_0]$ shifted by $\mathrm{Im}\left[c_{44}^{JT}(T_0)/c_0\right]_{mod}$; black curve is model curve calculated by formula (2) using fitting parameters listed in Table 2.

Insert in the upper right corner is evaluation of parameters in formula (5) using the peak model in Imaginary part: T_1=19.5 K;

$\mathrm{Im}[c^{JT}(T_1)/c_0]T_1$=0.00963.

Table 2. – Fitting parameters of simulation with three relaxation mechanisms

Crystal	$\mathrm{Im}[c^{JT}(T_1)/c_0]T_1$, K	τ_0, s	V_0, cm^{-1}	B^{-1}, sK	$B^{-1}\Theta^2$, sK^3
BaF_2:Cu	0.00963	$4\cdot10^{-11}$	66	$6.5\cdot10^{-7}$	$6\cdot10^{-5}$
$CaF_2:Cu^{2+}$[1]	0.562	$3\cdot10^{-12}$	118	$6.5\cdot10^{-7}$	$2\cdot10^{-3}$

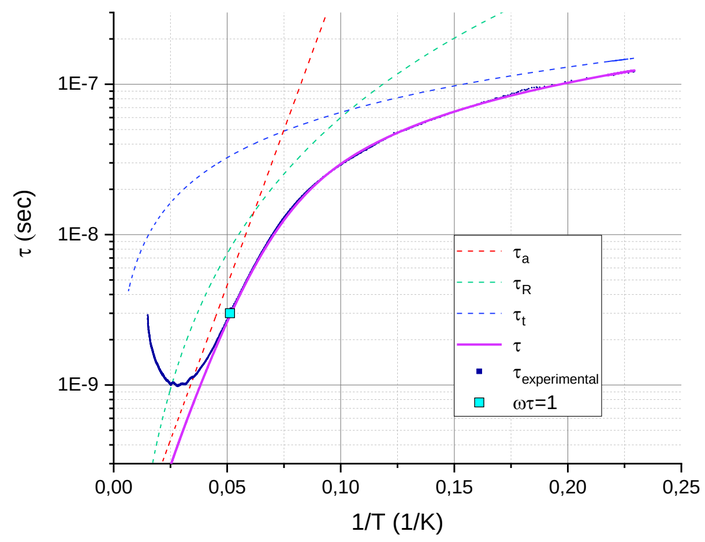

Fig.5 – Temperature dependences of relaxation time in the BaF_2:Cu crystal. Dark squares are experimental data, purple curve is total relaxation time modeled by three relaxation mechanisms. The blue square symbol corresponds to the condition $\omega\tau(T_1) = 1$.

Conclusion

Parameters of relaxation mechanisms determined in the present research can be used for comparison of the properties of the JT complexes in different host crystals and further calculation of the adiabatic potential energy surface parameters.

References

[1] M.N. Sarychev et al.; JETP 135 473 (2022).
[2] I. B. Bersuker; The Jahn-Teller Effect (2006).
[3] M.M. Zaripov, V.A. Ulanov *Sov. Phys. Solid State* **31** (1989).

The study was supported by the Ministry of Science and Higher Education of the Russian Federation (Ural Federal University Program of Development within the Priority-2030 Program).